

Relativistic Plasma Screening Effects on Pulsational Pair-Instability Supernova, ~~Magnetars~~, ~~Other Sites~~

M.A. Famiano¹⁻³, G. Mathews^{2,4}, A. Baha Balantekin^{2,5}, M.K. Cheoun⁶, T. Kajino^{2,3,7}, M. Kusakabe³, Y. Luo^{2,3,7}, T. Maruyama⁸, K. Mori^{2,3,7}, T. Suzuki⁸

¹Western Michigan University, ²National Astronomical Observatory of Japan, ³Beihang University, ⁴Notre Dame University, ⁵University of Wisconsin, ⁶Soongsil University, ⁷University of Tokyo, ⁸Nihon University

29 July 2021



Screening and Weak Interactions in High-T, High-B Plasmas

Outline

- 1 Introduction
- 2 Significance of Relativistic Effects
 - Statistics and Length Scales
 - Screening Lengths
- 3 Results: PPISN & PISN
 - Pulse Morphology
 - Black Hole Masses
 - Nucleosynthesis
- 4 Conclusions
- 5 Other Applications: Weak Interactions

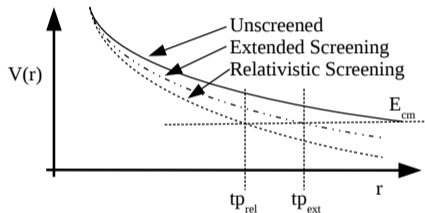
Published Preprints

- arXiv:2009.10925 - ApJ 904, 29 (2020)
- arXiv:2006.14148 - ApJ 898, 163 (2020)
- arXiv:2002.08636 - PRD 101, 083010 (2020)
- arXiv:1603.03137 - PRC 93, 045804 (2016)

Review: Nuclear Screening - Old Physics With New Applications

Plasmas Characterized by Debye Length: **Shorter Debye Length = More Screening**

Small shift in potential \rightarrow big shift in r_{tp}

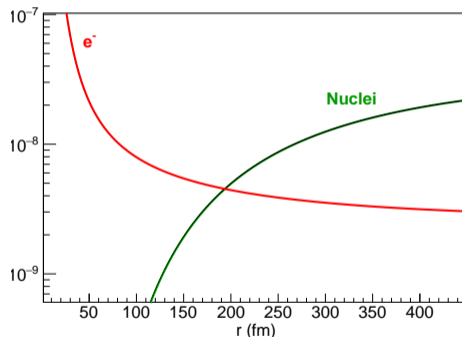


Weak Screening Length (Debye Length):

$$\phi_{scr}(r) = \frac{Ze}{r} e^{-\frac{r}{\lambda}}$$

$$\lambda \propto \frac{\partial n}{\partial \phi}$$

Charge Density vs. Radius



More charge means more enhanced screening, **regardless of the sign of the charge.**

For High Temperature in Plasma....

Everything starts with the charge density, n . (Electron charge densities shown.)

Classical Screening: MB Distribution

$$n = -Zn_ze \exp \left[-\frac{e\phi}{kT} \right]$$

Relativistic Screening: High-Temperature: Fermi-Dirac Screening

$$n = -\frac{e}{4\pi} \int_0^\infty d^3p \left[\frac{1}{e^{(E-\mu-e\phi)/T} + 1} - \frac{1}{e^{(E+\mu+e\phi)/T} + 1} \right]$$

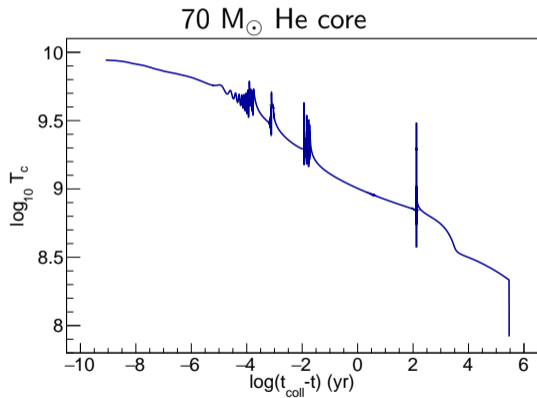
With B-Fields: Landau Levels

$$n = -\frac{eB}{2\pi^2} \sum_{\nu=0}^{\infty} g_\nu \int_0^\infty dp_z \left(\left[\exp \left(\frac{\sqrt{p_z^2 + m_e^2 + 2\nu eB} - \mu - e\phi}{T} \right) + 1 \right]^{-1} \right) - n_+$$

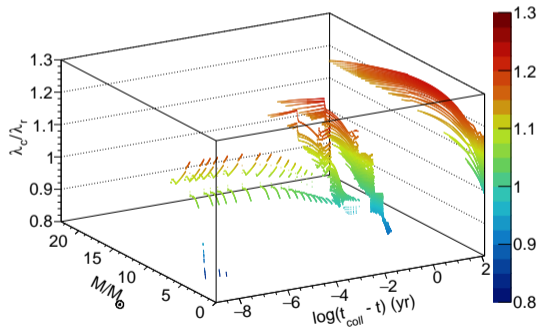
All of these change the Fermi-distribution, Pauli blocking factor, and λ_D .

Applicability of Relativistic Screening to PPISN

Ratio of Screening Lengths: MESA Time Steps **Larger $\lambda_c/\lambda_r \rightarrow$ More Enhanced Rates**



Each dot is a mass element at a time step.
Only $kT > 150$ keV shown.

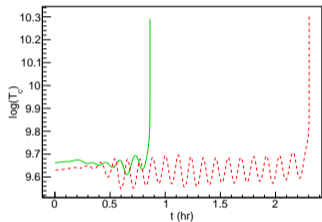


MESA simulations adapted from Marchant et al. (2019).

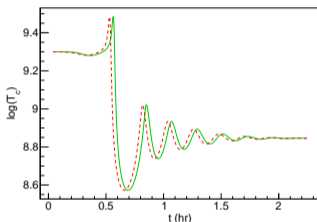
Pulse Morphology: First Pulse

First Pulse: 44, 44.5, 70, 76, 89, 89.02 M_{\odot} , Increased Heating, ^{16}O Burning

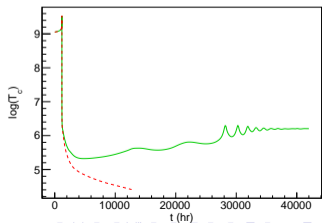
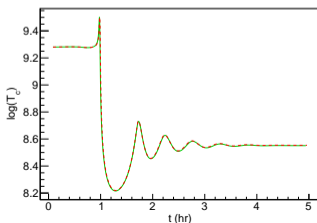
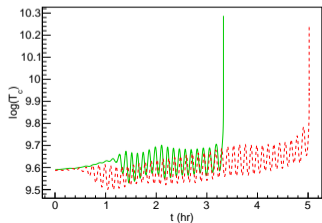
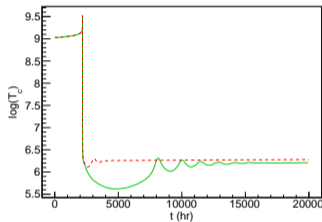
DC-PPISN Boundary



"Intermediate" M_{prog}

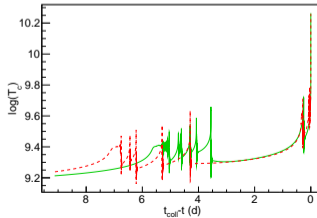
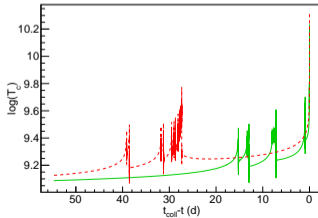
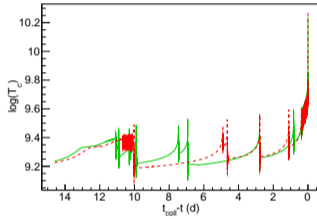
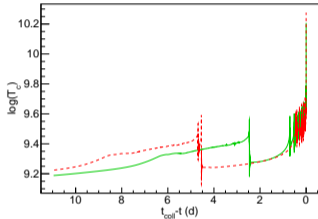


PPISN-PISN Boundary



Pulse Morphology: Last Pulse

Final Pulse: 52, 58, 64, 70 M_{\odot} He Core - Small Changes in Overall System Stability

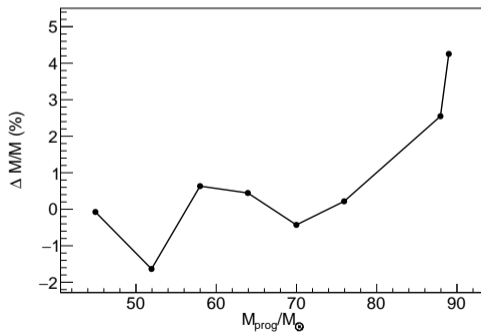
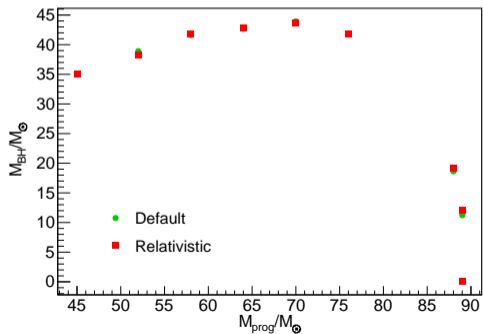


Instabilities

- Some changes in overall pulse morphology.
- NOTE: $t_c - t$: all final points set to zero.
- Pulsational phase can have slight increase in heating.
- System instability affects T_c where system leaves pulsational period.

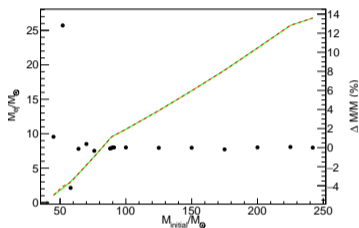
Black Hole Masses

Small change in BH mass and **slight** shift in PPISN-PISN boundary. However, **overall change is likely not greater than numerical uncertainties of model.**

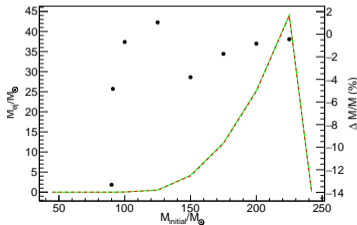
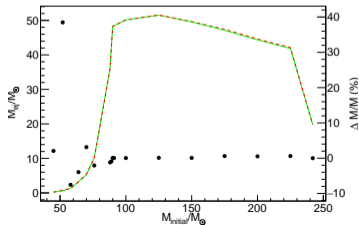
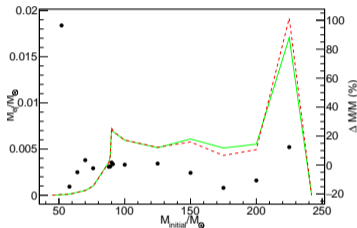


Nucleosynthesis and Ejecta

PISN: Winds (top: ^{12}C , bottom: ^{16}O)



PISN: Explosion (Top ^{56}Fe , bottom: ^{56}Ni)



Ejected Mass

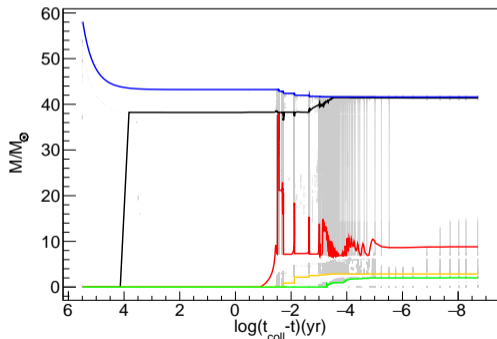
- Light elements: "Large" differences in pulsational ejections
- Little difference in PISN: Entire mass of star is ejected.
- Fe-group elements: Some difference in PISN ejection: Core burning.

Stellar Evolution

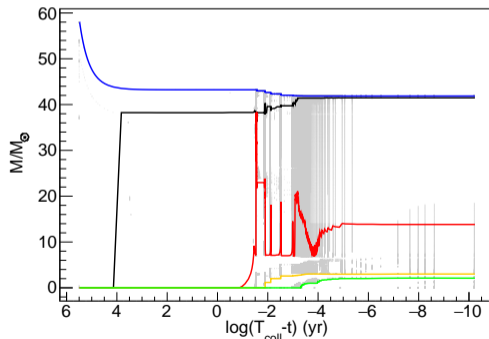
Kippenhahn Diagram: $58 M_{\odot}$ He Core, Surfaces defined where $X < 10^{-2}$.

He, C, O, Si

Note large convective region at pulsation. C/O boundary more extreme changes.



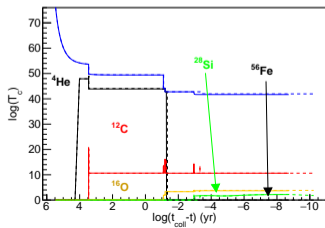
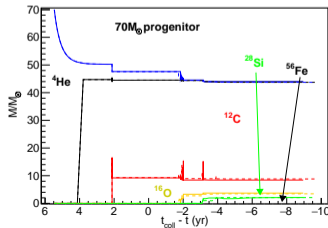
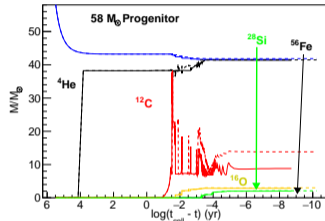
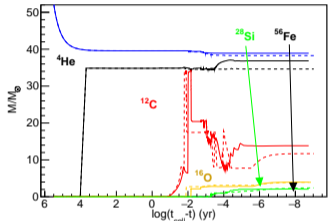
Classical screening.



Relativistic screening.

Stellar Evolution

Kippenhahn Diagrams: 52, 58, 70, 76 M_{\odot} He Core



Compare Diagrams

- Solid: Default, Dashed: Relativistic
- Mass loss (blue line) may differ slightly. Wind sensitivity for He shell.
- Differences in pulse periods (hot T)
- Largest sensitivity for C/O boundary in lighter stars.

Conclusions

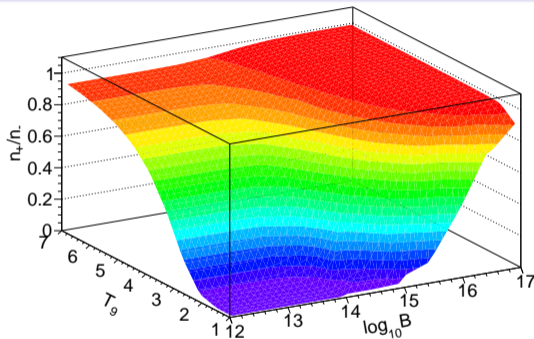
Conclusions

- Very little sensitivity of final black hole mass to screening model.
- Have not addressed strong screening yet. (Default screening in the core.)
- Some changes in ejected mass from increased heating, changes to core boundaries.
- Reduce temperature range of numerical model.
- Currently working on high B-fields in n-star and PNS cooling. Relevance to “lower” BH mass gap?
- Advertisement: Other sites include collapsar nucleosynthesis, BBN, magnetar surfaces. Weak rates and screening at high-B.

Work supported by NSF PHY-1204486 and PHY-1712832, NASA Grant #80NSSC20K0498 an NAOJ Visiting Professorship, and the Fulbright Program

Are Relativistic Effects Important?

Positron-Electron Ratios and Screening Length Ratios: More Charge \rightarrow More Screening

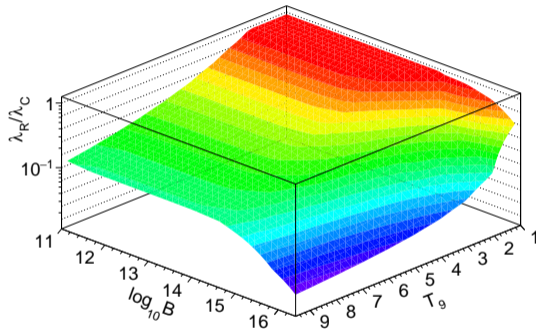


Positron/electron ratio vs. T_9 and B.

$\rho = 10^6 \text{ g cm}^3$, $Y_e = 0.5$.

Chemical potential changes.

Famiano et al., ApJ (2020)



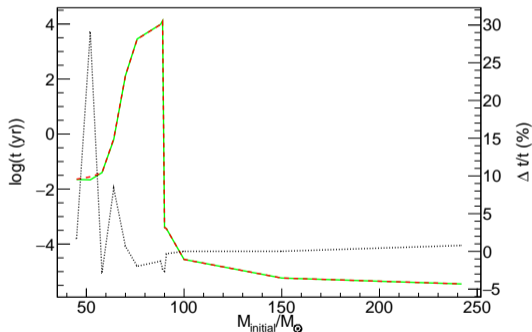
λ_R/λ_C vs. T_9 and B

(Note: just showing electron screening length only.)

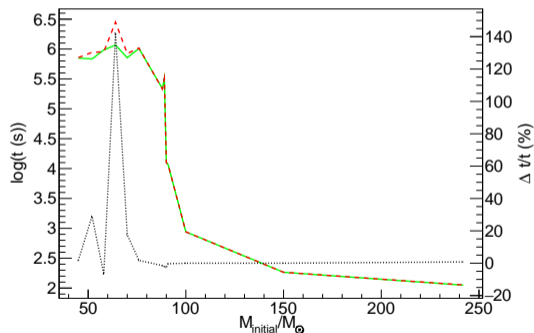
Shorter screening length \rightarrow Stronger Screening

Collapse Time

Overall trends reflect instabilities in models.



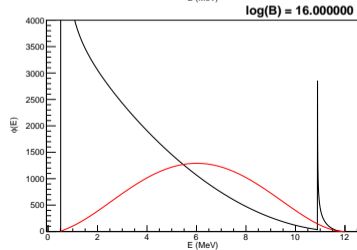
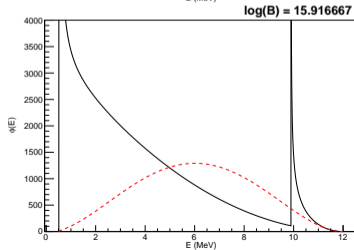
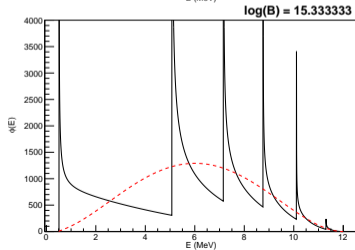
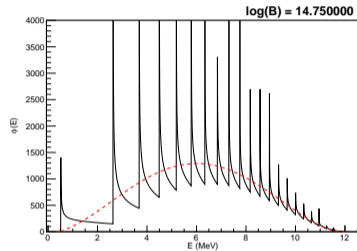
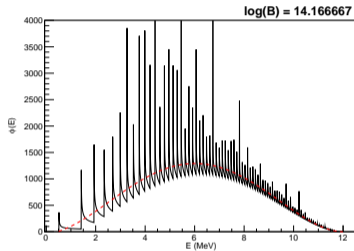
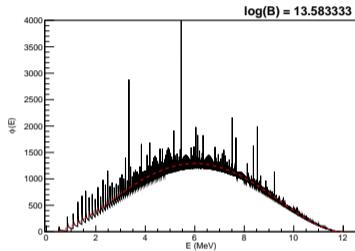
Total time from first pulse to collapse/explosion.



Total time at $kT > 150$ keV.

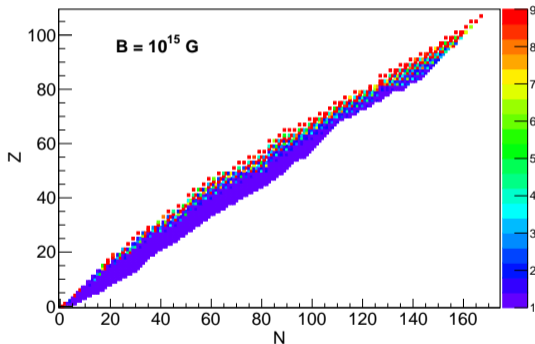
Beta-Decay Integrands

Electron Spectrum of β Decay for $Q=12$ MeV: Fermi Function and Pauli Blocking in Weak Interactions

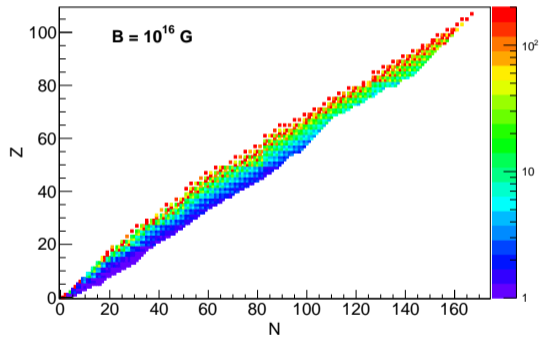


β^- -Decay Ratios in Collapsar Environment

$\rho = 10^6 \text{ g cm}^{-3}$, $Y_e = 0.5$, Fermi Theory...



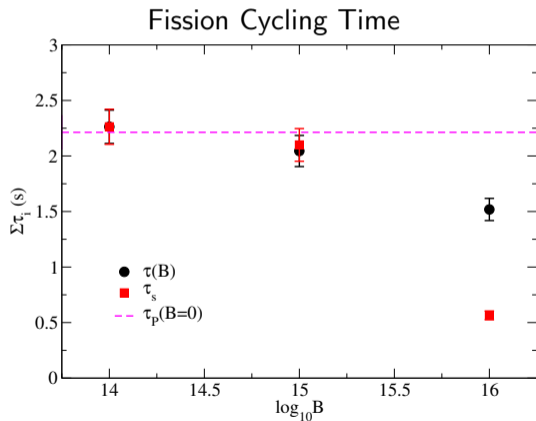
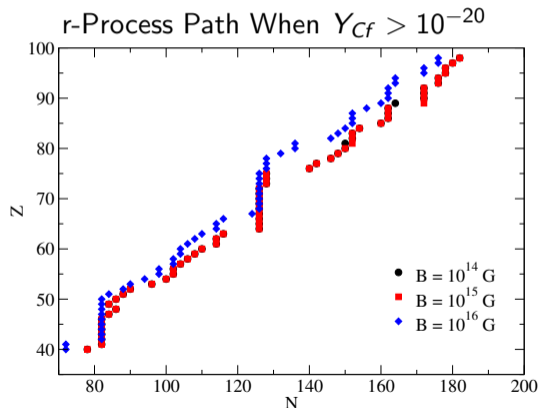
$eB \lesssim Q$: Little change.



$eB \gtrsim Q$: More significant change.

Increased Decay Rates Shift the r-Process Path (Collapsar Model)

Faster Decay Rates, Shift in Path, Also Fission Cycling Time Changes

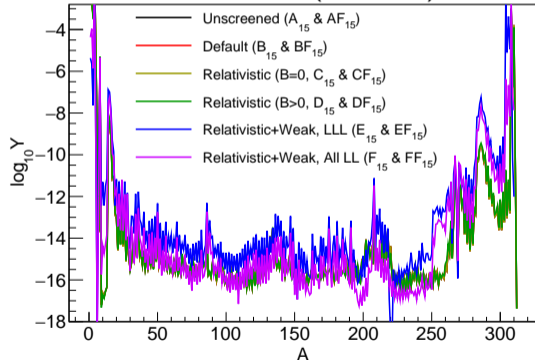


Famiano et al., ApJ (2020), Nakamura et al., A&A (2015)

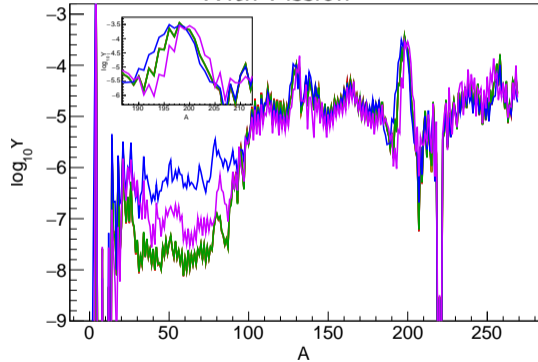
Collapsar Nucleosynthesis

r-Process Abundance Distribution, $B = 10^{15}$ G

Without Fission (Artificial)



With Fission



NOTE: Screening alone has little effect (n-capture = no Coulomb). Enhanced β rates has a noticeable effect, including shift in peaks. Fission is necessary!

Characterizing a Collapsar r-Process Site by Field and Fission

Galactic Chemical Evolution?

Sr/X Ratios

$$R \equiv \frac{(Y_{\text{Sr}}/Y_{\text{X}})_B}{(Y_{\text{Sr}}/Y_{\text{X}})_{B=0}}$$

- How do ratios change with B.
- Shifts can be dramatic as abundance peaks shift (e.g., Dy).
- Also heavily dependent on fission model.
- Can be used to characterize a single-site r-process?

